Malaysian Journal of Chemistry, 2023, Vol. 25(3), 354-367
(Special Issue: *3rd IKMPB Online Symposium 2023 - Innovation in Chemistry Towards Sustainable Development*)

Development of Ultraviolet Spectroscopic Method for the Estimation of Metronidazole Nanoparticles for Periodontal Disease Treatment

Nora Azirah Mohd Zayi[1], Muhammad Lutfi Mohamed Halim[1], Ahmad Fahmi Harun Ismail[1,2], Mohd Yusof Mohamad[1,2]

[1]Department of Physical Rehabilitation Science, Kulliyyah of Allied Health Sciences, International Islamic University Malaysia, Kuantan Campus, 25200 Kuantan, Pahang, Malaysia

[2]Cluster of Cancer Research Initiative IIUM (COCRII), International Islamic University Malaysia, Kuantan, 25000, Kuantan, Pahang, Malaysia

*Corresponding author (e-mail: yusofkahs@iium.edu.my)

In periodontitis treatment, metronidazole (MT) is applied topically to reduce systemic side effects and reach the target site. treatment of periodontitis via sustained MT release. The UV-spectrophotometer analysis was developed and validated to quantify the encapsulated MT according to ICH Q2 (R1) guidelines, which include parameters such as specificity, linearity, accuracy, precision (in the form of repeatability), the limit of detection (LOD) as well as the limit of quantification (LOQ), range, robustness, and ruggedness. Metronidazole nanoparticles (MT-NP) were fabricated at different concentrations (0.15–0.60 mg/mL) using ionic gelation. The encapsulated MT was examined using a UV spectrophotometer, a Nano Zetasizer, Fourier transform infrared spectroscopy (FTIR), and a field emission scanning electron microscope (FESEM). The maximum wavelength (max) was discovered to be 320 nm, and it obeyed Beer's law with a linear relationship (R^2 = 0.999) in the range of 2-12 µg/mL. The parameters analyzed met ICH Q2 (R1) standards. MT-NP had a spherical structure and absorption band similar to chitosan empty (CS), with a size of 308.0 ± 9.18 nm, a polydispersity index of 0.374 ± 0.37, 46.6 ± 0.23, and an encapsulation efficiency of 87.95 ± 0.07. These findings suggest that UV-visible can be a useful tool for the estimation of MT nanoparticles and MT-NP as promising local antibacterial agents to treat periodontitis.

Keywords: Metronidazole nanoparticle; UV/Vis spectroscopy; local drug delivery; eriodontal disease

Received: January 2023; Accepted: April 2023

Periodontal disease, also known as periodontitis, is a serious dental health problem where, according to the Global Burden Disease Study (2019), about 14.5% of the global population suffers from severe periodontal disorders. Periodontal disease causes redness, swelling, gingival pain, and bad breath, and if left untreated, the development of a periodontal pocket occurs, where the gum tissue pulls away from the tooth. Patients with low innate ability often experience slow regeneration of healthy periodontal tissue, which worsens the disease due to bacteria accumulation. These microorganisms can damage the periodontal gum, alveolar jaw, and other supporting tooth structures, which can lead to tooth loss [1]. Periodontal disease is caused by poor oral hygiene, stress, aging, alcohol, depression, smoking, and systemic conditions such as cardiovascular disease and diabetes [1, 2]. The data collected showed that periodontal disease is linked to the buildup of *Porphyromonas gingivalis*, *Treponema denticola*, *Fusobacterium nucleatum*, *Aggregatibacter actinomycetemcomitans*, *Prevotella intermedia*, and *Tannerella forsythia*. These species are present in subgingival plaque in patients suffering from chronic periodontitis [3]. The presence of *Porphyromonas gingivalis* and *Treponema denticola*, which have been demonstrated to exhibit synergistic virulence in animal models, was found to be significantly correlated with the development and severity of chronic periodontitis. Another study found that *Tannerella forsythia* is also one of the bacteria that inhabit the subgingival cavity and initiates connective tissue and alveolar bone degeneration [4]. Among them is *Porphyromonas gingivalis*, a gram-negative anaerobic bacterium prevalent in the oral cavity. It secretes hydrolytic, proteolytic, lipolytic, and toxic metabolites [5].

In the early stages of periodontal disease, non-surgical treatments, including scaling and root planing, as well as local or systemic antibiotics, are the most successful treatments. In chronic periodontitis, several systemic antibiotic therapies such as tetracyclines, penicillin, metronidazole, or clindamycin are early approaches to minimizing infections after dental surgery. Among the antibiotics used, metronidazole (MT) is a

†Paper presented at the 3rd IKMPB Online Symposium 2023 - Innovation in Chemistry Towards Sustainable Development

periodontal antibiotic that is commonly used to treat periodontitis due to its broad-spectrum activity and efficacy against obligate anaerobes [6]. Metronidazole (C6H9N3O3) [2-(2-methyl-5-nitro1H- imidazol-1-yl) has antibacterial, antiparasitic, and anticancer properties. It was widely used against anaerobic bacteria and certain parasites caused by Trichomonas vaginalis, Entamoeba histolytica, and Giardia lamblia, and deep-sited infections in different organs such as various brain, pulmonary, and pelvic anaerobes [7]. Over the last 60 years, metronidazole, a nitroimidazole, has remained a preferred drug for inflammatory disorders associated with the gastrointestinal tract, including colitis caused by Clostridium difficile. In 1962, while treating the protozoan Trichomonas vaginalis in vaginitis, MT was effective in treating gingivitis. Until recently, MT was considered an excellent choice for Clostridium difficile and periodontitis. MT has the advantage of being rapidly absorbed by humans, which results in a high level of biological activity against anaerobic bacteria [8]. However, MT has a half-life of six to eight hours, causing side effects like nausea, abdominal cramps, and a metallic taste [9]. Furthermore, MT resistance develops after long-term oral administration, limiting their use. Unlike traditional local drug delivery, which results in rapid and burst release over a short period, this limitation can be addressed by nanotechnology, which allows the drug to be released over long periods while also allowing the drug to penetrate regions inaccessible to large particles [10]. As a result, researchers have focused their efforts on developing nanoantibiotics, that can reach the target site while avoiding systemic side effects.

Previously, the potential systemic application of metronidazole nanoparticles was studied in the treatment of colon and gut infections. However, different approaches and attempts have been proposed to obtain the desired nanoparticle with ideal particle size, polydispersity index, and stability, primarily for systemic application in colon disease; consequently, in this study, we discussed and formulated the metronidazole nanoparticle that is well suited for local periodontal disease treatment. In this study, CS was used to prepare nanoparticles and load MT. Even though chitosan's solubility limits its use in biological applications, chitosan has several advantageous properties that make it a preferred material for many applications in biomedical and biomaterials research, as well as nanoparticle technology. Many types of chitosan derivatives are nontoxic, biocompatible, and biodegradable and were classified as GRAS (generally recognized as safe) by the Food and Drug Administration (FDA) [11]. It also has high permeability toward biological membranes, is cost-effective, and has antimicrobial activities [12]. Furthermore, chitosan nanoparticles can boost the immune system’s ability to fight cancer [13]. Chitosan-based nanocarriers can be formed through various methods such as hydrogen bonds, Van der Waals interactions, including hydrophobic and electrostatic interactions, or monomer polymerization emulsions, cross-linking, spray drying, and the reverse micellar method [11, 14]. Because of its ease of formulation, high biocompatibility, biodegradability, safety for human use, and high permeability toward biological membranes, chitosan was used as a drug carrier in this study. In this study, CS nanocarriers were formed using an ionic gelation technique. It is based on the ionic interaction between the positively charged amino groups of chitosan and the negatively charged groups of a polyanion, which is also called a cross-linker. Sodium tripolyphosphate (STTP) is the most common crosslinker used to develop CS nanoparticles because it is safe and has beneficial properties. Polyphosphates like STTP are broken down into simpler phosphates, which are considered healthy, low-toxic, and generally regarded as safe. It has also been reported that STTP poses no carcinogenic or mutagenic risks [14]. In the development of chitosan-based nanocarriers, it is crucial to quantify the amount of drug successfully encapsulated. Thus, it is important to develop a simple, sensitive, accurate, precise, and repeatable yet precise and robust analytical method for the estimation of MT encapsulated in a chitosan nanocarrier [10]. We used a UV spectrometer to assess the presence of MT encapsulated in chitosan in this study. All analysis parameters were done following ICH Q2 (R1) guidelines and were statistically validated using the relative standard deviation (%RSD) value [15, 16]. Despite the various advantages acquired from the use of HPLC chromatography, it does have drawbacks such as the high cost of instrumentation and operation, relatively long analytical duration, and the need for experience in handling the equipment and processing samples [17]. Thus, the UV spectrophotometer is a highly convenient analytical technique due to its simplicity, reproducibility, and low cost [18]. MT-NP were fabricated by ionic interaction following the development and validation of UV-spectrophotometer analysis. Chitosan nanoparticles were employed to load MT due to their good physiochemical properties in drug delivery systems [19]. Therefore, the objectives of the present study were to develop and validate the UV spectrophotometer analysis as well as to obtain nano-sized MT-NP. Metronidazole-loaded chitosan nanoparticles are synthesized through ionic gelation and thus can be measured using a UV spectrophotometer.

MATERIAL AND METHODS

1. Method Development and Validation

A simple, precise, and rapid UV spectrophotometric analytical method for post-fabrication of metronidazole nanoparticles was developed to confirm that the analytical procedure employed is suitable for identifying and quantifying substances of interest. Thus, this research develops and validates the spectrophotometric method according to International Conference on Harmonization (ICH) Q2 (R1) guidelines. The guidelines provide all the detailed parameters to perform the analytical method and analysis, which included specificity, linearity, accuracy, precision (in the form of repeatability), the limit of detection (LOD)

as well as the limit of quantification (LOQ), range, and robustness [16]. The validation procedures consist of specific characteristic parameters that must meet a certain acceptance criterion to make the analytical method acceptable.

1.1. Specificity

A simple, precise, and rapid UV spectrophotometric analytical method for post-fabrication of metronidazole nanoparticles was developed to confirm that the analytical procedure employed is suitable for identifying and quantifying substances of interest. Thus, this research develops and validates the spectrophotometric method according to International Conference on Harmonization (ICH) Q2 (R1) guidelines. The guidelines provide all the detailed parameters to perform the analytical method and analysis, which included specificity, linearity, accuracy, precision (in the form of repeatability), the limit of detection (LOD) as well as the limit of quantification (LOQ), range, and robustness [16]. The validation procedures consist of specific characteristic parameters that must meet a certain acceptance criterion to make the analytical method acceptable.

1.2. Linearity and Calibration Curve

The aliquots of concentration, ranging from 2–12 µg/mL were prepared in triplicates. The calibration curve concentration vs. absorbance was plotted and subjected to least squares regression analysis, yielding the equation y = mx + c, and the R2 was established. The concentration of the analyte was determined using the notations "x" and "y" as the absorbance values. The correlation coefficient R2 value for all the standard curves constructed must not be less than 0.995 as one of the acceptance criteria.

1.3. Precision

There is a need to ascertain that the time variation does not influence MT concentration measurement. Thus, in this study, the precision of the assay method was assessed in terms of repeatability via intraday and interday measurements by subjecting three concentration levels of MT (8 µg/ml, 10 µg/mL, and 12 µg/mL to the same wavelength. Intraday precisions were measured by analyzing the three prepared samples at three different specific time points on the same day, and interday precisions were measured on three consecutive days, respectively. The precision was calculated using the percentage relative standard deviation (% RSD), which had to be less than 2.0% to meet the acceptance criteria.

$$\%\ RSD\ =\ (standard\ deviation\ of\ measurements\ /\ mean\ value\ of\ measurements)\ x\ 100 \quad (1)$$

1.4. Accuracy (Recovery)

For accuracy, three different concentrations of MT (8 µg/ml, 10 µg/mL, and 12 µg/mL) were subjected to a wavelength of 320 nm, and the experimental concentrations were recorded in triplicate, as well as the mean and standard deviation. The accuracy was calculated using the percentage recovery from the calibration curve. The following equation was used to calculate the percentage recovery. The percentage recovery should not be less than 98% or more than 102%, indicating the method was accurate.

$$\%\ Recovery\ =\ (Amount\ found/Amount\ added)\ x\ 100 \quad (2)$$

1.5. Robustness

The robustness of the analysis shows its reliability with respect to deliberate variations in method parameters. The method was evaluated by making a small change either in the procedures or sample preparations. In this study, robustness was tested by adjusting the wavelength by ± 2 nm from the set wavelength. The absorbance of an 8 µg/mL concentration was measured in triplicate at two different wavelength conditions, and the result is presented in % RSD, as shown in equation (1).

1.6. Ruggedness

The ruggedness was carried out using two different instruments (Secomam UVline 9400 and UV-1800, Shimadzu). The UV-spectrophotometer method was performed by analyzing seven samples of MT. The results are presented in % RSD, as shown in equation (1).

1.7. Limit of Detection (LOD) and Limit of Quantification (LOQ)

The limit of quantification (LOQ) of an analytical procedure is the lowest amount of drug in a sample that can be quantitatively determined with suitable precision and accuracy. To determine the LOD and LOQ of MT, the solution was prepared in triplicate near the lower limit of the analytical curve and subjected to the same wavelength to quantify the samples. The limit of detection (LOD) and limit of quantification (LOQ) of MT were determined using the standard deviation of the response (S.D.), referring to the S.D. of the sample and slope (m) obtained from the calibration curve constructed and calculated according to equation (3) and (4) described below:

$$LOD\ =\ 3.3(S.D./m) \quad (3)$$

$$LOQ\ =\ 10\ (S.D./m) \quad (4)$$

2. Fabrication of Metronidazole Nanoparticles

Metronidazole (99% purity) was purchased from Xi'an Henrikang Biotech, China; chitosan (CS) was purchased from Xi'an Ceres Biotech, China; and sodium tripolyphosphate (STTP) and acetic acid were purchased from Evachem, Selangor, Malaysia. Nanoparticles were prepared using the ionic gelation method previously described in the literature with a slight modification: chitosan was dissolved in 2% (v/v) aqueous acetic acid. Subsequently, metronidazole was added to the chitosan solution. STTP solution (0.1% w/v) was dissolved in distilled water and added dropwise to the chitosan-metronidazole solution for 60 min at 800 rpm. The final mixture was centrifuged at 1,500 rpm for 30 minutes. Finally, metronidazole-loaded chitosan nanoparticles were collected and freeze-dried for 24 hours at -80 °C to obtain the powdered nanoparticle. Similarly, the blank chitosan nanoparticles were prepared following the above process without adding metronidazole, according to a previous study with a slight modification [20, 21].

2.1. Particle Size, PDI, and Zeta Potential

The size and PDI (polydispersity index) of MT-NP were measured by the dynamic light scattering (DLS) technique using the Nano Zetasizer (Malvern). All measurements were obtained in triplicate (n = 3) [19].

2.2. Drug Encapsulation Efficiency (EE)

The encapsulation efficiency of the MT nanoparticle was determined by an indirect method. Briefly, the nanoparticle was centrifuged at 1,500 rpm for 30 minutes. The amount of MT in nanoparticles was calculated as the difference between the total amount used to prepare the nanoparticles and the amount of MT present in the supernatant (non-encapsulated MT). The concentration of free MT, as shown in Figure 1, was determined by UV-spectrophotometry, and EE nanoparticles were calculated as follows in triplicate [20, 22].

2.3. Formulation Selection of MT-NP

The optimal nanoparticle formulations were optimized using the one variable at a time (OVAT) approach. The formulation resulted in the smallest particle size, the lowest PDI value, a zeta potential greater than +20 mV, and the highest encapsulation efficiency of metronidazole, which were selected for further study. For this purpose, different formulations were prepared by varying the concentration of MT from 0.15–0.60% (w/v), which will be discussed later [21].

2.4. Field Emission Scanning Electron Microscope (FESEM)

The surface morphology of optimized MT-NP was analyzed to observe the shape and aggregation phenomena. The nanoparticle was fixed on a glass plate and dried at room temperature. The dry nanoparticle was coated with gold under a vacuum and then analyzed using field emission scanning electron microscopy (FESEM) [23].

$$\%\, EE = (drug\ concentration\ in\ the\ formulation - drug\ concentration\ in\ the\ supernatant) / drug\ concentration\ in\ the\ formulation \quad (5)$$

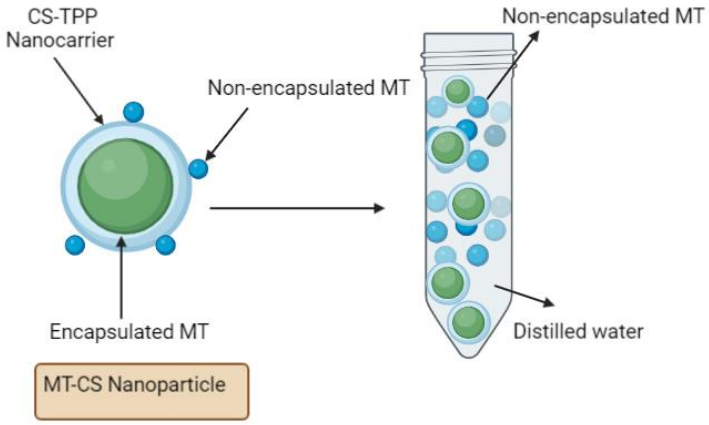

Figure 1. The λ max of MT using a spectrophotometer at 320 nm.

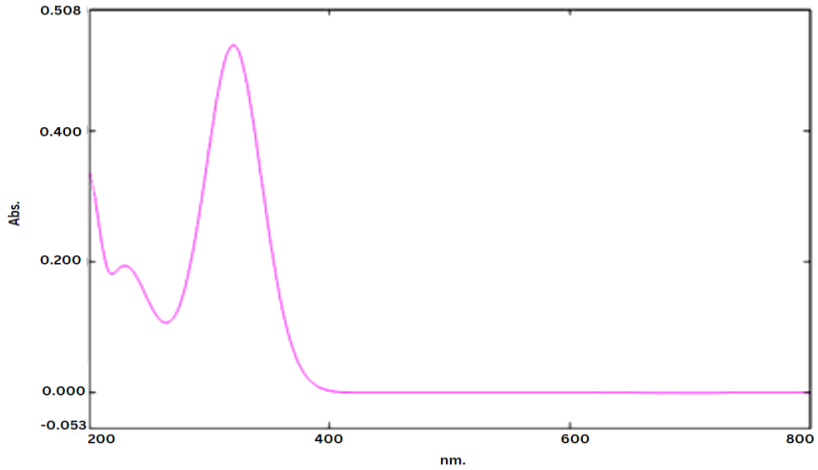

Figure 2. The λ max of MT using a spectrophotometer at 320 nm.

2.5. Attenuated Total Reflectance Fourier Transform Infrared Spectroscopy (ATR-FTIR)

A small quantity of MT-NP was scanned in the spectral region of 4,000 cm-1 to 400 cm-1 using ATR-FTIR (Perkin Elmer, Massachusetts, USA) [24].

RESULTS AND DISCUSSION

Analytical Procedure and Validation

Validation of an analytical procedure refers to the process of verifying and documenting that an analytical method is suitable for its intended use. The validation process involves demonstrating that the analytical procedure is accurate, precise, specific, and robust for its intended application. It is an essential step in ensuring that the results obtained from the analytical method are reliable.

1.1 Analytical Procedure and Validation

As stated in a previous study, chitosan is water-insoluble due to strong intermolecular hydrogen bonds between polymer chains, and drug release from CS is driven by swelling, drug diffusion, degradation, or a combination of both [11, 13]. The CS nanocarrier that dissolves upon contact with the media causes an explosive effect on the drug trapped, which may fail the nanosystem. As a result, the insoluble nanocarrier is an important feature for nanoparticle formulation because it can provide a slow release of encapsulated drugs. In this study, chitosan was used as the primary carrier in the nanosystems and was also shown to be insoluble in water. Because CS can only disperse in water, they effectively act as nanocarriers, preventing rapid drug release and promoting MT release via nanocarriers. As a result, long-term control of MT release at the site of action is possible. Furthermore, the interaction between two oppositely charged polymers, CS and STPP, leads to more hydrogen bond formation, causing the outer layer of nanocarrier CS-STPP to swell in the water system due to strong hydrogen bonds between polymers. As the pH rises, the CS-STPP swells, preventing the nanocarrier structure from breaking [25]. However, a study found that the solubility of CS can be reduced due to entanglement with a polymeric matrix in an acidic medium [21]. Thus, CS-STPP was not included in the specificity because it is insoluble in water. The result showed that only one peak presents in the spectrum with a maximum wavelength of 320 nm, which belongs to metronidazole. According to Figure 2, an absorbance value less than one is adequate for measuring the wavelength of the maximum absorbance (λ max) of MT [26].

1.2. Linearity and Calibration Curve

The peaks of MT detected at 320 nm showed linear regression data at a six-point range of MT concentrations ranging from 2 to 12 g/mL, obeying Beer's law. Table 1 shows the concentrations versus mean absorbance values of MT. The linearity study revealed that the developed UV method was linear with a correlation coefficient of 0.999, as shown in Figure 3. The method was regarded as robust if the R2 values obtained were not less than 0.995 [27]. As a result of these findings, the analytical method for quantifying MT was found to be robust.

Table 1. Means absorbance of metronidazole (n = 3 ± S.D.).

Metronidazole (ug/mL)	Mean Absorbance (nm)
2	0.139 ± 0.006
4	0.228 ± 0.015
6	0.313 ± 0.011
8	0.424 ± 0.011
10	0.510 ± 0.007
12	0.606 ± 0.004

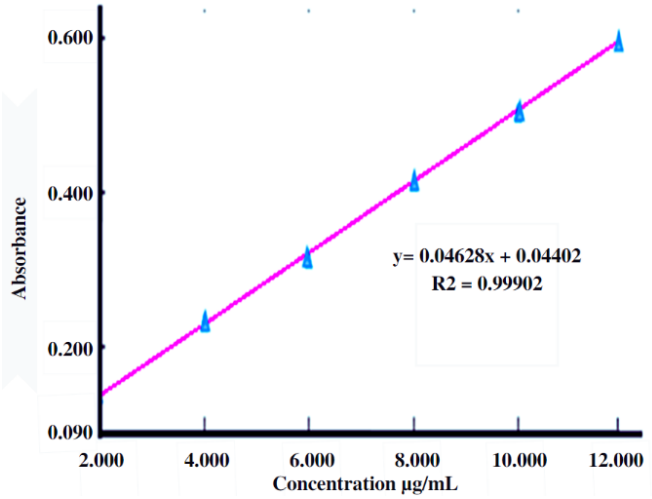

Figure 3. Calibration curve between absorbance vs concentration of MT.

A calibration curve is a graphical representation of the relationship between the concentration or amount of a substance being measured and the signal response obtained from an analytical instrument. Once the calibration curve is established, an unknown sample can be analyzed using the same analytical method, and its signal response is compared to the calibration curve to determine the concentration or amount of the substance in the sample. This is done by interpolating the signal response of the unknown sample onto the calibration curve to obtain the corresponding concentration. According to Beer's Lambert Law, absorbance is proportional to concentration, allowing the instrument to predict the concentration of an analyte in a sample [28]. As a result, the calibration curve can be used to estimate the number of encapsulated MT nanoparticles. The calibration curve was plotted at λmax (320 nm) by constructing a graph between absorbance and concentrations, as shown in Figure 3.

1.3. Precision

The precision of a measurement can be expressed as a standard deviation or a coefficient of variation, which is the ratio of the standard deviation to the mean. The smaller the standard deviation, or the coefficient of variation, the higher the precision. It implies that for the measurements, or an analytical procedure, to be considered reliable, the result must be reproducible. A precise analytical method leads to accurate results, and a precise analytical procedure yields accurate results [29]. Considering the importance of reproducible yet accurate results, intra- and inter-day precision were established at 8, 10, and 12 µg/mL levels of MT using a UV spectrophotometer. The results in terms of mean absorbance values and % RSD for the intra- and inter-day precision studies are demonstrated in Tables 2 and 3. The precision (intraday and interday measurements) results demonstrated good reproducibility, with a percent relative standard deviation (% RSD) less than 2.0 and meeting the precision acceptance criteria.

Table 2. Intraday- precision (n = 3 ± S.D.).

Time	Concentration µg/mL	Mean absorbance (nm)	% RSD
9 am	8	0.456 ± 0.008	1.754
	10	0.525 ± 0.008	1.524
	12	0.627 ± 0.009	1.435
12 pm	8	0.458 ± 0.008	1.746
	10	0.518 ± 0.004	0.772
	12	0.615 ± 0.004	0.650
3 pm	8	0.460 ± 0.002	0.435
	10	0.534 ± 0.002	0.375
	12	0.627 ± 0.011	1.754

Table 3. Interday- precision (n=3± S.D.).

Day	Concentration	Mean absorbance (nm)	% RSD
1	8	0.438 ± 0.006	1.369
	10	0.516 ± 0.003	0.581
	12	0.610 ± 0.008	1.311
2	8	0.460 ± 0.002	0.435
	10	0.534 ± 0.002	0.375
	12	0.627 ± 0.011	1.754
3	8	0.438 ± 0.004	0.913
	10	0.516 ± 0.010	1.938
	12	0.593 ± 0.010	1.686

1.4. Accuracy

The accuracy of a measurement can be expressed as a percentage or an absolute value, such as the difference between the measured value and the true value. It is often evaluated by comparing the results obtained from the experiment to a known standard or reference material. The accuracy of an analytical method is an important parameter in chemical analysis, as it determines the reliability and validity of the results obtained. The accuracy of samples was assessed to evaluate the known impurity level following ICH Q2 (R1) guidelines. A minimum of nine determinations, consisting of three concentration levels and three replicates per sample, were conducted. The result was expressed as a percent recovery and should be between 98% and 102% [30]. The result showed that drug recoveries of 99.73–101.92% were obtained at concentrations of 8 µg/mL–12µg/mL. Based on the results, the developed UV method was found to be highly accurate, as the percentage recovery was within the standard range.

1.5. Robustness

The robustness of analytical methods measures the method's ability to remain unaffected when slight intentional changes in method parameters occur. In this study, the robustness of the UV spectrophotometer analytical method was established by reading the absorbance at a different wavelength. Change in wavelength did not affect the method's performance, as the % RSD values at 318 nm and 322 nm were found to be between 0.581 and 0.749, respectively, as shown in Table 4. The robustness of the proposed UV analytical method was demonstrated by a value of % RSD less than two.

Table 4. Robustness (n = 3 ± S.D.).

Wavelength	Mean Absorbance (nm)	%RSD
318	0.516 ± 0.003	0.581
322	0.534 ± 0.004	0.749

Table 5. Ruggedness (n = 3 ± S.D.).

Instrument	Mean Absorbance (nm)	% RSD
UV line 9400**,** Secomam	0.626 ± 0.0077	1.230
UV-1800, SHIMADZU	0.617 ± 0.0049	0.794

1.6. Ruggedness

The ruggedness of an analytical method is the degree of reproducibility of test results obtained by the analysis of the same samples under different test conditions. This study used two different UV spectrophotometers in different laboratories and at different times to test the analytical method's ruggedness. The results obtained from lab-to-lab and time-to-time variation were reproducible, as the %RSD did not exceed 2%, as shown in Table 5.

1.7. Limit of Detection and Limit of Quantification

LOD, or limit of detection, is the lowest amount of analyte that can be reliably detected by an analytical method. This is typically defined as the concentration or amount of analyte that produces a signal that is significantly different from the background noise of the method. In other words, it's the smallest amount of a substance that can be detected with any certainty. LOQ, or limit of quantification, is the lowest amount of analytes that can be accurately quantified or measured by an analytical method. This is typically defined as the concentration or amount of analyte that produces a signal that is reliably different from the background noise of the method and falls within an acceptable range of uncertainty. In other words, it's the smallest amount of a substance that can be accurately measured with a specific degree of confidence. LOD and LOQ were calculated using standard calibration curves. LOD and LOQ were found to be 0.040 µg/mL and 0.120 µg/mL, respectively, indicating that the method was suitable for analyzing samples containing even a small amount of MT.

2. Development of Chitosan-Loaded Metronidazole Nanoparticles

Chitosan, being a multivalent cationic polysaccharide, forms gels with suitable anions. Sodium tripoly-phosphate was used in this study as a counterion to chitosan. Chitosan is insoluble in alkaline and neutral pH solutions but soluble in acidic solvents. The protonated amine groups interact with phosphate ions, provided by STPP, either by intermolecular or intra-molecular linkage. In addition of the chitosan solution to the STPP solution, the acetic acid of the chitosan solution is rapidly neutralized with the ingress of coagulation fluid, which causes a decrease in pH within the beads. Simultaneously, the amine group of chitosan interacts with the phosphate ions of the tripolyphosphate solution. Both processes lead to the precipitation of chitosan with the simultaneous entrapment of added metronidazole within its matrix [31].

2.1. Particle size, PDI, and Zeta Potential

In this study, the relationship between the independent metronidazole (drug) concentration and three dependent variables, particle size (PS), polydispersity index (PDI), and entrapment efficiency (%EE), was studied. There were significant changes in size, PDI, and stability at different concentrations of MT. The MT nanoparticle was successfully synthesized by employing the ionic-crosslinking approach with a particle size range of 308.0 ± 9.184–600.5 ± 22.47 nm. Table 6 shows a linear relationship between the particle size of MT and the CS-STPP ratio, where an increase in the MT results in an increase in the particle size. The result depicts a previous study where the particle size increased with an increase in MT concentration at a constant CS-STPP concentration [24]. This is because more CS-STPP is required to trap the drug, and after the chitosan molecules are fully crosslinked with STPP, the excess formation of a single particle (MT) will result in large particle size [14].

In a previous study, it was found that when a higher proportion of STPP was used, the nanoparticles formed a neutral charge [20]. As in this study, chitosan (0.3% w/v) was used at a higher concentration than STPP (0.1% w/v), thus forming a positive charge zeta potential between 26.6 ± 6.100 and 46.6 ± 0.231 mV due to the higher polycation of chitosan. It may be said that the availability of protonated amino groups is higher with increasing concentrations of chitosan [32]. The decrease in zeta potential charge with increasing drug concentration demonstrated that this was most likely due to the non-encapsulated MT bond to the outer layer of CS-STPP crosslinking, which impedes zeta potential reading. The particle size distribution depends on several factors, such as the CS-STPP mixing, the chitosan concentration, the degree of deacetylation and molecular weight, the ionic strength, and the media. CS-STPP nanoparticles are usually polydisperse and suffer from poor stability, which limits their use. In this study, the nanoparticle size distribution was determined using the DLS technique through the polydispersity index (PDI) value. No data mention the criteria for an acceptable PDI for nanoparticle drugs in oral applications. In previous studies, PDI values ranging from 0.01 to 0.5–0.7 formed monodispersed particles, whereas a PDI Index value of 0.7 indicated a broad particle size distribution

of a nanoparticle system formulation. A PDI value of 0.1, on the other hand, is considered highly monodispersed, whereas a PDI value greater than 0.4 and a value in the range of 0.1–0.4 indicate that the system has a moderately dispersed distribution in the respective order [33]. All the batches of nanoparticles exhibit PDI index values of 0.374 ± 0.625–0.625 ± 0.083, which range from moderately monodisperse to highly polydisperse. As the nanoparticle formulated in this study increases with the increase of MT, it is due to the amount of STPP in the polyanion that fully interacts with the amino groups of chitosan to form a gel through inter- and intra-molecular cross-linkages during the ionic gelation procedure [14]. Thus, this caused the formation and precipitation of a single particle of CS in the obtained nanoparticle, which caused the increase in the PDI value [20].

2.2. Encapsulation Efficiency

The encapsulation of the drug within a nanocarrier is one of the success criteria of nanoparticles as therapeutic agents. The greater the efficacy of encapsulation, the greater the amount of drug entrapped in the carrier system. The percentage of drug efficiency MT ranged from 26.42–87.95%, as shown in Table 6. The greater the efficacy of encapsulation, the greater the amount of drug entrapped in the carrier system. The drug entrapment was shown to decrease with a rising concentration of MT at a constant concentration of 0.3% (w/v) chitosan, suggesting a relationship between drug entrapment and polymer concentration. This is due to enough polymer being required for the drug to be entrapped [34]. As a result, more chitosan is required to capture more drugs at high MT concentrations [9, 35].

2.3. Selection of MT-NP

Even though previous studies have been done to produce metronidazole nanoparticles using ionic gelation, many factors, such as the degree of deacetylation and molecular weight of chitosan, the CS-STPP mixing, the concentration of CS and TPP, the ionic strength, the stirring speed, the rate of TPP addition, and the freeze-drying method, may affect the final nanoparticle product [14]. Because there are so many variables that involve and affect the final nanoparticle product, we used the one variable at a time (OVAT) method by adopting the previous methodology with modifications to MT ratios and finding their effect on the particle size, polydispersity index, and stability while keeping other parameters constant. MT concentrations ranging from 0.15 to 0.60% (w/v) were prepared while other parameters and CS-STTP concentrations remained constant. Furthermore, a previous study focused on metronidazole nanoparticles being delivered selectively in the colon region through the oral route [24, 35]. This is the first study that will discuss the potential of metronidazole nanoparticles for periodontal local drug delivery. CS nanocarriers were chosen for this study because they have a longer residence time at the site of application, can harmonize their release kinetics or charge, and improve their mucoadhesive properties. The ability to adhere to mucosal surfaces or mucoadhesion has attracted much attention in the last few decades. Not only can they adhere to mucosal tissues, but they also offer increased surface area and enhanced bioavailability by protecting the drug from degradation. This adhesive property is considered valuable for pharmaceutical purposes, as mucosal drug delivery has great potential to improve drug absorption and bioavailability through mucosal membranes [36]. Thereby, it increases the adhesion to the mucosa and, as a result, enhances the time of contact for penetration of drug molecules [37]. The movement of nanoparticles to the affected area in periodontal disease is depicted in Figure 4 below.

Table 6. Physicochemical properties of nanoparticles (n = 3 ± S.D.).

No	Independent variable		Dependent variable			
	Chitosan polymer (%w/v)	Drug (%w/v)	Size (nm)	PDI (nm)	Zeta Potential (mV)	EE%
F1	0.3	0.15	308.0 ± 9.18	0.374 ± 0.37	46.6 ± 0.23	87.95 ± 0.07
F2	0.3	0.30	594.2 ± 14.7	0.479 ± 0.04	35.6 ± 0.40	85.06 ± 0.08
F3	0.3	0.45	746.9 ± 13.7	0.581 ± 0.08	26.6 ± 6.10	35.79 ± 0.42
F4	0.3	0.6	600.5 ± 22.4	0.625 ± 0.08	32.9 ± 0.87	26.42 ± 1.35

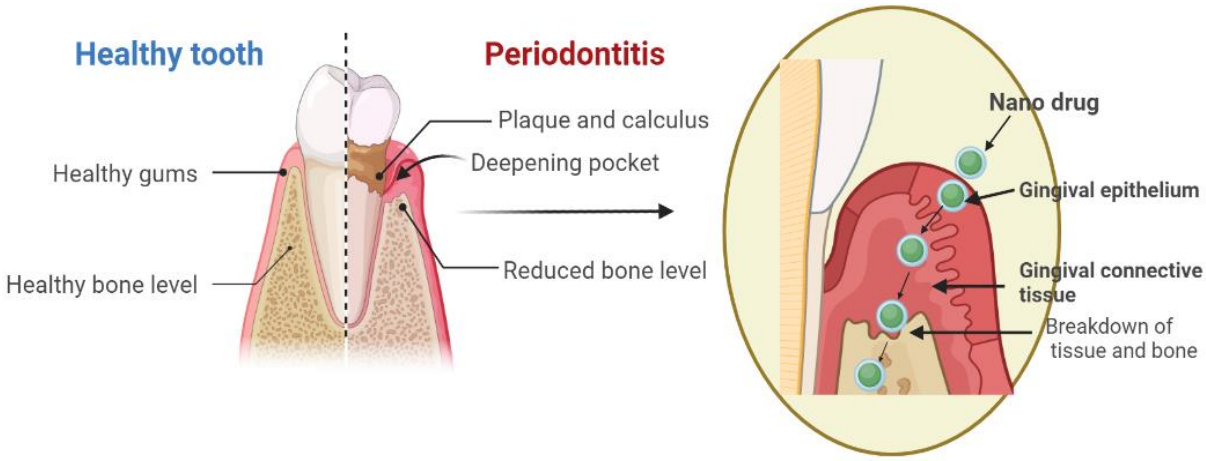

Figure 4. The nano-drug flow to the area affected by periodontal disease created with BioRender.

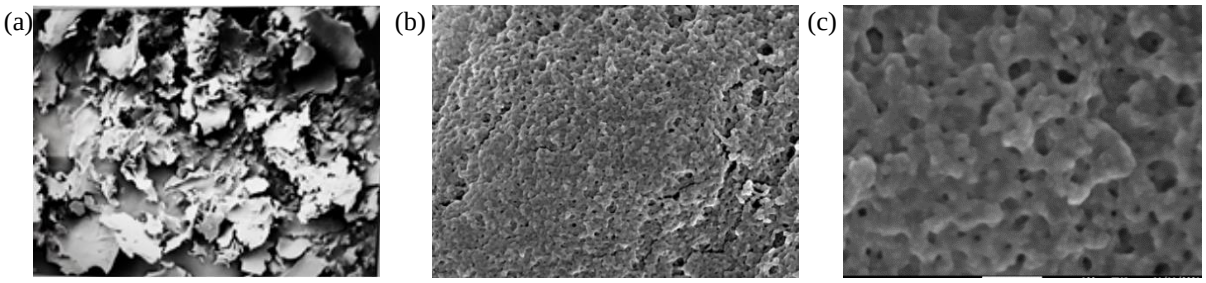

Figure 5. Images of CS (a) and MT-NP (b-c).

The particle size was one of the key variables that needed to be controlled at the nanoscale (1–1,000 µm) to be recognized as a nanoparticle and suitable for application in the treatment of periodontal disease. Delivering a therapeutic agent across the gingival sulcus to the underlying connective tissue should be a key desirable property for any ideal drug delivery system intended for the localized treatment of periodontal disease. According to a previous study, particles that are larger than 500 nm in diameter may not permeate through the junctional epithelium to deliver the drug at the site of action [38]. Thus, in this study, the optimal nanoparticle formulations were chosen based on particle sizes less than 500 nm. Figure 4 shows the nano-drug flow to the area affected by periodontal disease. Secondly, the PDI value reflects the nanoparticle size distribution, where samples with a wider range of particle sizes have higher PDI values, while samples consisting of an evenly distributed particle size distribution have lower PDI values [39]. In our studies, a lower PDI value of 0.374 ± 0.374 was observed, indicating monodisperse chitosan nanoparticles. Meanwhile, all of the formulated materials have a zeta potential greater than +20 mV and the highest encapsulation efficiency in this study is 87.95 ± 0.07%. Based on the experiment findings, formulation number three (F3) achieved favorable results for all the responses at a chitosan concentration of 0.3% w/v and a metronidazole concentration of 0.15% w/v, with the smallest particle size of 308.0 ± 9.184 nm, the lowest PDI of 0.374 ± 0.374, the highest zeta potential, and the highest encapsulation efficiency of 87.95 ± 0.07%. Thus, F3 was selected as the optimal formulation based on the capability of formulation-produced nanoparticles with the desired size, PDI zeta potential, and entrapment efficiency for periodontal local drug delivery.

2.4. Encapsulation Efficiency

The image in Figure 5 depicts pure chitosan as captured by a Field Emission Scanning Electron Microscope (FESEM); the images depict chitosan in the form of flakes. This is similar to a previous study that found that the original chitosan was also in flakes, whereas the chitosan nanoparticles were round [40]. As shown in many studies, drugs loaded onto chitosan nanocarriers presented a round shape and a distinct spherical, solid surface with a porous structure [20, 21, 41], while the SEM images of an empty CS nano-particle showed the spherical-like structure in the agglomerated state [12]. Similar morphology was found in this study, where the selected MT-NP exhibited a uniform distribution and spherical-like structure in large clumps, which indicated the MT-NP were successfully formulated. The observed matrix structure of nanoparticles was formed due to the electrostatic force of attraction between an anionic

group and a cationic group of CS [21]. Furthermore, agglomeration was observed in MT-NP in the dry state, and as mentioned in previous studies, agglomeration has been considered the primary phenomenon for the synthesis of novel chitosan nanoparticles for biomedical applications and nanomedicine [12].

3. ATR-FTIR Analysis

The interaction between metronidazole and the chitosan polymer was studied using ATR-FTIR. Figure 6 shows the MT-NP spectrum is similar to that of pure CS nanoparticles; only the differences between the IR spectra were seen in the wavenumbers for the wavelengths that were shifted to higher or lower frequencies. The wavenumber shift is due to the cross-link formed between the STTP. No formation of a new peak was observed in the ATR-FTIR of the MT-NP. As stated in the previous study, encapsulation of ascorbic acid in poly(lactic-co-glycolic) acid PLGA nanoparticles were successful from the absence of all the peaks of ascorbic acid in the FTIR spectra of PLGA nanoparticles [42]. Thus, in this study, the successful encapsulation of MT in the CS nanocarrier could be demonstrated from the absence of the peaks of metronidazole in the FTIR spectra of MT-NP, as shown in Figure 6. Likewise, there were no changes in the surface charge of the nanoparticles. This indicates that the drug did not interfere with the intermolecular bonds between CS and STPP, maintaining the stability of nanoparticles [20].

The current method for quantifying MT using UV spectroscopy was validated following the ICH Q2 (R1) guidelines. The proposed analytical method was found to be precise, linear, specific, robust, and rugged, fulfilling all acceptance criteria. Thus, the developed UV method was applied for the estimation of MT content in CS nanocarriers. In a previous study, antibiotics loaded into nanocarriers could be released slowly while maintaining necessary concentrations at the target site, and the ideal drug delivery system should be able to transport active compounds safely to the intended site of action. In periodontal disease, the ideal drug delivery should make optimal contact with the mucosal surfaces in the periodontium, prolong the residence time in the pocket, and intensify contact with the junctional epithelium [43]. This strategy is important to improve the regeneration ability of damaged tissues and to effectively treat periodontal disease. Thus, nanotechnology drug delivery approaches are highly promising in achieving these goals. It provides an advantage where therapeutic molecules could be encapsulated or loaded in carriers, such as nanoparticles or scaffolds, to allow targeted, sustained, and controlled release of the molecule to the intended location [44]. The metronidazole nanoparticles synthesized in this study were successfully encapsulated in a chitosan nanocarrier with satisfactory particle size and high zeta potential and stability, which made them ideal for periodontal use. Although further in vitro and in vivo research is needed to assess the efficacy of MT nanoparticles as a therapy for periodontal disease, our current results demonstrate that these MT nanoparticles have the potential to be used in this application. Nanoparticles loaded with metronidazole, which is a beneficial candidate antibacterial drug incorporated into the GBR membrane to prevent infection, should have a significant effect on bone regeneration; thus, a future study will investigate the effects of MT loaded into the GBR membrane on tissue regeneration.

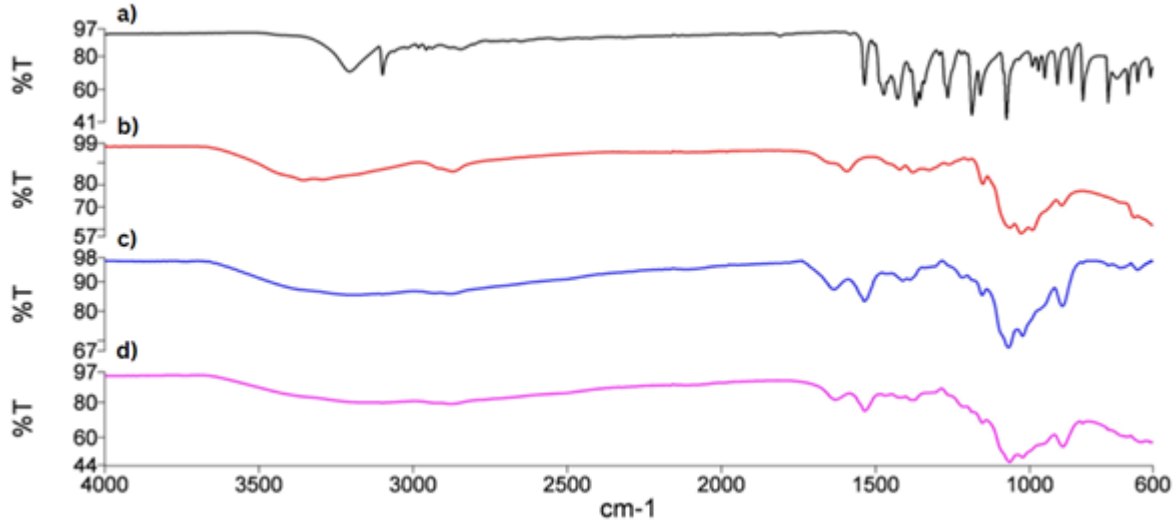

Figure 6. ATR-FTIR images of MT (a), CS (b), CS nanoparticle (c), and MT-NP nanoparticle (d).

CONCLUSION

The quantification method for metronidazole content in chitosan nanocarriers was developed and validated using UV spectrophotometry. This study fulfilled all the acceptance criteria according to ICH Q2 (R1) guidelines. The data collected herein supported the use of this analytical method for the quantification of nanosized MT in vitro assessments due to its rapidity, precision, specificity, accuracy, robustness, ruggedness, and cost-effectiveness. Furthermore, it was demonstrated that nanosized MT could be successfully fabricated using an ionic gelation method potentially used for periodontal disease treatment. However, further in vitro and in vivo studies will be conducted to examine the antibiotic's efficiency against periodontal disease.

ACKNOWLEDGEMENTS

The authors would like to acknowledge the Malaysian Ministry of Higher Education for the financial support provided by the FRGS19-146-0755 grant.

REFERENCES

1. Arigbede, A. O., Babatope, B. O., Bamidele, M. K. (2012) Periodontitis and systemic diseases: A literature review. *J Indian Society of Periodontology*, **16**, 487–491.

2. Nazir, M. A. (2018) Prevalence of periodontal disease, its association with systemic diseases and prevention. *International Journal of Health Sciences (Qassim)*, **11**, 72–80.

3. Chukkapalli, S. S., Rivera-Kweh, M. F., Velsko, I. M., Chen, H., Zheng, D., Bhattacharyya, I., Gangula, P. R., Lucas, A. R., Kesavalu, L. (2015) Chronic oral infection with major periodontal bacteria Tannerella forsythia modulates systemic atherosclerosis risk factors and inflammatory markers. *Pathogen and Disease*, **73**, 1–12.

4. Tan, K. H., Seers, C. A., Dashper, S. G., Mitchell, H. L., Pyke, J. S., Meuric, V., Slakeski, N., Cleal, S. M., Chambers, J. L., McConville, M. J. and Reynolds, E. C. (2014) Porphyromonas gingivalis and Treponema denticola exhibit metabolic symbioses. *PLoS pathogens*, **10(3)**, p.e1003955.

5. How, K. Y., Song, K. P., Chan, K. G. (2016) Porphyromonas gingivalis: An overview of periodontopathic pathogen below the gum line. *Frontier in Microbiology*, **7**, 1–14.

6. Dodwad, V., Vaish, S., Mahajan, A., Chhokra, M. (2012) Local drug delivery in periodontics: A strategic intervention. *International Journal of Pharmacy and Pharmaceutical Sciences*, **4**, 30–34.

7. Alawadi, D. Y., Saadeh, H. A., Kaur, H., Goyal, K., Sehgal, R., ben Hadda, T., Elsawy, N. A., Mubarak, M. S. (2015) Metronidazole derivatives as a new class of antiparasitic agents: Synthesis, prediction of biological activity, and molecular properties. *Medicinal Chemistry Research*, **24**, 1196–1209.

8. Dingsdag, S. A., Hunter, N. (2018) Metronidazole: An update on metabolism, structure-cytotoxicity and resistance mechanisms. *Journal of Antimicrobial Chemotherapy*, **73**, 265–279.

9. Garud, A., Garud, N. (2010) Preparation and evaluation of chitosan microcapsules of metronidazole using tripolyphosphate cross-linking method. *Dhaka University Journal of Pharmaceutical Sciences*, **9**, 125–130.

10. Zhang, J., Ma, S., Liu, Z., Geng, H., Lu, X., Zhang, X., Li, H., Gao, C., Zhang, X., Gao, P. (2017) Guided bone regeneration with asymmetric collagen-chitosan membranes containing aspirin-loaded chitosan nanoparticles. *International Journal of Nanomedicine*, **12**, 8855–8866.

11. Herdiana, Y., Wathoni, N., Shamsuddin, S., Muchtaridi, M. (2022) Drug release study of the chitosan-based nanoparticles. *Heliyon*, **8**, e08674.

12. Oh, J. W., Chun, S. C. & Chandrasekaran, M. (2019) Preparation and in vitro characterization of chitosan nanoparticles and their broad-spectrum antifungal action compared to antibacterial activities against phytopathogens of tomato. *Agronomy*, **9(1)**, 21.

13. Bashir, S. M., Ahmed Rather, G., Patrício, A., Haq, Z., Sheikh, A. A., Shah, M. Z. U. H. & Fonte, P. (2022) Chitosan Nanoparticles: A Versatile Platform for Biomedical Applications. *Materials*, **15(19)**, 6521.

14. Al-Nemrawi, N. K., Alsharif, S. S. M., Dave, R. H. (2018) Preparation of chitosan-tpp nanoparticles: The influence of chitosan polymeric properties and formulation variables. *International Journal of Applied Pharmaceutics*, **10**, 60–65.

15. Agency, E. M. (2011) European Medicines Agency: An unacceptable choice. *Prescrire International*, **20**, 278.

16. European Medicines Agency ICH (2005) Q2 (R1): Validation of analytical procedures: text and methodology. *International Conference on Harmonization*, **2**, 1–15.

17. Siqueira-Moura, M. P., Primo, F. L., Peti, A. P. F., Tedesco, A. C. (2010) Validated spectrophotometric and spectrofluorimetric methods for determination

of chloroaluminum phthalocyanine in nanocarriers. *Pharmazie*, **65**, 9–14.

18. Darwish, I. A., Amer, S. M., Abdine, H. H., Al-Rayes, L. I. (2009) New spectrophotometric and fluorimetric methods for determination of fluoxetine in pharmaceutical formulations. International Journal of Analytical Chemistry, **2009**, 1–9.

19. Katas, H., Raja, M. A. G. & Lam, K. L. (2013) Development of chitosan nanoparticles as a stable drug delivery system for protein/siRNA. *International Journal of Biomaterials*, **2013**.

20. Oliveira, A., Araújo, A., Rodrigues, L. C., Silva, C. S., Reis, R. L., Neves, N. M. & Martins, A. (2022) Metronidazole delivery nanosystem able to eeduce the pathogenicity of bacteria in colorectal infection. Biomacromolecules, **23(6)**, 2415-2427.

21. Sukhbir, K., Chawla, V., Narang, R. K., Aggarwal, G. (2017) Comparative mucopenetration ability of metronidazole loaded chitosan and pegylated chitosan nanoparticles. *Asian Journal of Pharmaceutical and Clinical Research*, **10**, 125–130.

22. Jackson, T. C., Agboke, A. A., Udofa, E. J., Ucheokoro, A. S., Udo, B. E., Ifekpolugo, N. L. (2019) Characterization and release kinetics of metronidazole loaded silver nanoparticles prepared from carica papaya leaf extract. *Advance in Nanoparticle*, **08**, 47–54.

23. Patel, B. K., Parikh, R. H., Aboti, P. S. (2013) Development of oral sustained release rifampicin loaded chitosan nanoparticles by design of experiment. *Journal of Drug Delivery*, **2013**, 1–10.

24. Kandav, G., Bhatt, D. C., Jindal, D. K. (2019) Formulation and evaluation of allopurinol loaded chitosan nanoparticles. *International Journal of Applied Pharmaceutics*, **11**, 49–52.

25. Mohammed, M. A.., Syeda, J. T. M., Wasan, K. M, Wasan, E. K. (2017) An overview of chitosan nanoparticles and its application in non-parenteral drug delivery. *Pharmaceutics*, **9(4)**, 53.

26. Mondal, N., Pal, T. K., Ghosal, S. K. (2007) Development and validation of a spectrophotometric method for estimation of letrozole in bulk and pharmaceutical formulation. *Pharmazie*, **62**, 597–598.

27. Ismail, A. F. H., Mohamed, F., Rosli, L. M. M., Shafri, M. A. M., Haris, M. S., Adina, A. B. (2016) Spectrophotometric determination of gentamicin loaded PLGA microparticles and method validation via ninhydrin-gentamicin complex as a rapid quantification approach. *Journal of Applied Pharmaceutical Science*, **6**, 007–014.

28. Delgado, R. (2022) Misuse of Beer–Lambert Law and other calibration curves. *Royal Society Open Science*, **9(2)**, 211103.

29. Mishra, A. K., Kumar, A., Mishra, A. & Mishra, H. V. (2014) Development of ultraviolet spectroscopic method for the estimation of metronidazole benzoate from pharmaceutical formulation. *Journal of Natural Science, Biology, and Medicine*, **5(2)**, 261.

30. Ismail, A. F. H., Mohamed, F., Mansor, N., Shafri, M. A. M. & Yusof, F. A. (2015) Method development and validation using UV spectrophotometry for Nigella sativa oil microparticles quantification. *Journal of Applied Pharmaceutical Science*, **5(9)**, 082–088.

31. Srinatha, A., JK, P. & Singh, S. (2008) Ionic cross-linked chitosan beads for extended release of ciprofloxacin: in vitro characterization. *Indian Journal of Pharmaceutical Sciences*, **70(1)**, 16.

32. Kaur, S., Narang, R. K. & Aggarwal, G. (2017) Formulation and development of colon-targeted mucopenetrating metronidazole nanoparticles. *Tropical Journal of Pharmaceutical Research*, **16(5)**, 967–973.

33. Danaei, M., Dehghankhold, M., Ataei, S., Hasanzadeh Davarani, F., Javanmard, R., Dokhani, A. & Mozafari, M. R. (2018) Impact of particle size and polydispersity index on the clinical applications of lipidic nanocarrier systems. *Pharmaceutics*, **10(2)**, 57.

34. Sujathan, P, Sharma, U. K. (2021) Development and characterization of metronidazole loaded microsponges for the management of diabetic foot. *International Journal of Research and Review*, **8**, 440–457

35. Sreeharsha, N., Rajpoot, K., Tekade, M., Kalyane, D., Nair, A. B., Venugopala, K. N. & Tekade, R. K. (2020) Development of metronidazole loaded chitosan nanoparticles using QbD approach—A novel and potential antibacterial formulation. *Pharmaceutics*, **12(10)**, 920.

36. Eliyahu, S., Aharon, A. & Bianco-Peled, H. (2018) Acrylated chitosan nanoparticles with enhanced mucoadhesion. *Polymers*, **10(2)**, 106.

37. Mikušová, V. & Mikuš, P. (2021) Advances in chitosan-based nanoparticles for drug delivery. *International Journal of Molecular Sciences*, **22(17)**, 9652.

38. Aminu, N., Chan, S. Y. & Toh, S. M. (2018) Formulation design and optimization of triclosan loaded nanoparticles for enhanced drug delivery across gingival sulcus by Resolution IV modeling of Design Expert®. *Journal of Biomedical and Clinical Sciences (JBCS)*, **3(1)**, 83–90.

39. Masarudin, M. J., Cutts, S. M., Evison, B. J., Phillips, D. R. & Pigram, P. J. (2015) Factors determining the stability, size distribution, and cellular accumulation of small, monodisperse chitosan nanoparticles as candidate vectors for anticancer drug delivery: application to the passive encapsulation of [14C]-doxorubicin. *Nanotechnology, Science and Applications*, **11**, 67–80.

40. Vaezifar, S., Razavi, S., Golozar, M. A., Karbasi, S., Morshed, M. & Kamali, M. (2013) Effects of some parameters on particle size distribution of chitosan nanoparticles prepared by ionic gelation method. *Journal of Cluster Science*, **24**, 891–903.

41. Nesalin, J. A. J. & Smith, A. A. (2013) Preparation and evaluation of stavudine loaded chitosan nanoparticles. *Journal of Pharmacy Research*, **6(2)**, 268–274.

42. Hamdi, N. A. M., Haris, M. S. & Ismail, A. F. H. ( )The positive impact of vitamin C (Ascorbic Acid) utilisation in cancer treatment: A scoping review of published articles from the perspective of the in vitro studies. *Malaysian Journal of Medicine and Health Sciences*, **17**, 275–284.

43. Abou Neel, E. A., Bozec, L., Perez, R. A., Kim, H. W. & Knowles, J. C. (2015) Nanotechnology in dentistry: prevention, diagnosis, and therapy. *International Journal of Nanomedicine*, **10**, 6371.

44. Aminu, N., Chan, S. Y. & Toh, S. M. (2017) Roles of nanotechnological approaches in periodontal disease therapy. *Journal of Applied Pharmaceutical Science*, **7(7)**, 234–242.